Eur. J. Mineral.
2017, **29**, 129–141
Published online 14 October 2016

Gauthierite, $KPb[(UO_2)_7O_5(OH)_7]\cdot 8H_2O$, a new uranyl-oxide hydroxy-hydrate mineral from Shinkolobwe with a novel uranyl-anion sheet-topology

Travis A. OLDS[1], Jakub PLÁŠIL[2,*], Anthony R. KAMPF[3], Radek ŠKODA[4], Peter C. BURNS[1,5], Jiří ČEJKA[6], Vincent BOURGOIN[7] and Jean-Claude BOULLIARD[7]

[1] Department of Civil and Environmental Engineering and Earth Sciences, University of Notre Dame, Notre Dame, IN 46556, USA
[2] Institute of Physics ASCR, v.v.i., Na Slovance 1999/2, 18221 Prague 8, Czech Republic
*Corresponding author, e-mail: plasil@fzu.cz
[3] Mineral Sciences Department, Natural History Museum of Los Angeles County, 900 Exposition Boulevard, Los Angeles, CA 90007, USA
[4] Department of Geological Sciences, Faculty of Science, Masaryk University, Kotlářská 2, 611 37 Brno, Czech Republic
[5] Department of Chemistry and Biochemistry, University of Notre Dame, Notre Dame, IN 46556, USA
[6] Department of Mineralogy and Petrology, National Museum, Cirkusová 1740, 193 Prague 9, Czech Republic
[7] Association Jean Wyart, Collection des Minéraux de Jussieu, IMPMC, Université Pierre et Marie Curie, case courrier 73, 4 place Jussieu, 75252 Paris Cedex 05, France

Abstract: Gauthierite, $KPb[(UO_2)_7O_5(OH)_7]\cdot 8H_2O$, is a new uranyl-oxide hydroxy-hydrate mineral from the Shinkolobwe Mine, Democratic Republic of Congo, Africa. It occurs on a matrix of uraninite-bearing quartz gangue associated with soddyite and a minor metazeunerite–metatorbernite series mineral. It is a product of oxidation–hydration weathering of uraninite. Gauthierite is monoclinic, $P2_1/c$, with $a = 29.844(2)$ Å, $b = 14.5368(8)$ Å, $c = 14.0406(7)$ Å, $\beta = 103.708(6)°$, $V = 5917.8(6)$ Å^3 and $Z = 8$. Prismatic crystals have pronounced lengthwise striations and reach about 1 mm in length. Gauthierite is yellowish orange with a light orange streak and vitreous lustre. The Mohs hardness is ~3 to 4. It is brittle with an uneven fracture and perfect cleavage on {0 1 0}. The calculated density based on the empirical formula is 5.437 g/cm^3. Optically, gauthierite is biaxial (−), with $\alpha = 1.780(5)$, $\beta = 1.815(5)$, $\gamma = 1.825(5)$ (white light), $2V_{meas.} = 58(1)°$; dispersion is extreme ($r \gg v$). The optical orientation is $X = \mathbf{b}$, $Y \approx \mathbf{a}^*$, $Z \approx \mathbf{c}$ (or $X = \mathbf{b}$, $Y \wedge \mathbf{a} = 14°$ in obtuse β); it is pleochroic with X very pale yellow, Y and Z orange-yellow; $X \ll Y \approx Z$. Electron microprobe analyses (average of 9) provided: K_2O 1.29, PbO 7.17, UO_3 82.10, H_2O 8.78 (structure), total 99.34 wt.%. The empirical formula (based on 34 O *a.p.f.u.*) is: $K_{0.67}Pb_{0.78}U_7O_{34}H_{23.77}$. The ideal formula is $KPb[(UO_2)_7O_5(OH)_7](H_2O)_8$, which requires K_2O 1.90, PbO 9.00, UO_3 80.74, H_2O 8.35, total 100 wt.%. Raman and infrared spectral data confirm the presence of UO_2^{2+}, OH^- and molecular H_2O. The eight strongest powder X-ray diffraction lines are [d_{obs} in Å (hkl) I_{rel}]: 7.28 (020,400) 49, 3.566 (040, −802, −204) 67, 3.192 (622, −224) 100, 2.541 (−842, −244) 18, 2.043 (406) 14, 2.001 (662, −264, 14·2·0) 23, 1.962 (426, −146) 14, and 1.783 (12·0·4, −10·4·6) 17. The crystal structure of gauthierite ($R = 0.0567$ for 6997 reflections with [$I > 3\sigma(I)$]) contains uranyl-(hydroxo)-oxide sheets with a novel topology that is similar to that of vandendriesscheite, but with a unique chain sequence **UDPDPDUPUP**, $P_4(UD)_6$. Adjacent sheets are linked through K^+ and Pb^{2+} cations (the lone $6s^2$ pair on Pb atoms is stereoactive).

Key-words: gauthierite; new mineral; uranyl-oxide hydroxy-hydrate; crystal structure; topology; oxidation zone; Shinkolobwe.

1. Introduction

Uranyl-oxide hydrox-hydrate minerals play a key-role in initial alteration stages of primary U^{4+} minerals, such as uraninite, and are common constituents of the oxidized portions of uranium deposits worldwide (Finch & Ewing, 1992; Finch & Murakami, 1999; Krivovichev & Plášil, 2013). Uraninite alteration is also important because it is a natural analogue for spent nuclear fuel, SNF (Janeczek *et al.*, 1996). Gauthierite is a new member of this mineral family, which now consists of twenty-one species. The crystal structures of most of these species have been solved (see Table 1); only the structures of paulscherrerite (Brugger *et al.*, 2011) and heisenbergite (Walenta & Theye, 2012) remain unknown.

Here, we present a description of a new mineral from the Shinkolobwe mine (Katanga, Congo, Africa), gauthierite (/go ti: 'ei ait/). It is named in honour of Gilbert Joseph Gauthier (1924–2006), a famous Belgian geologist, mineralogist, and a true connoisseur of Katanga minerals (King, 2006). The new mineral and its name were approved by the Commission on New Minerals, Nomenclature and

0935-1221/17/0029-2586 $ 5.85
DOI: 10.1127/ejm/2017/0029-2586

Table 1. Selected anion topologies of structural units in uranyl-oxide minerals.

Anion topology	Sequence	U:O	Mineral	Chemical formula	Reference
α-U_3O_8	[PD]	3:5	–	U_3O_8	[1]
			Protasite	$Ba[(UO_2)_3O_3(OH)_2](H_2O)_3$	[2]
			Billietite	$Ba[(UO_2)_6O_4(OH)_6](H_2O)_8$	[3]
			Becquerelite	$Ca[(UO_2)_3O_2(OH)_3]_2(H_2O)_8$	[4]
			Richetite	$(Fe,Mg)_xPb_{8.57}[(UO_2)_{18}O_{18}(OH)_{12}]_2(H_2O)_{41}$	[5]
			Agrinierite	$K_2(Ca_{0.65}Sr_{0.35})[(UO_2)_3O_3(OH)_2]_2(H_2O)_5$	[6]
			Masuyite	$Pb[(UO_2)_3O_3(OH)_2](H_2O)_3$	[7]
			Compreignacite	$K_2[(UO_2)_3O_2(OH)_3]_2(H_2O)_7$	[8]
β-U_3O_8	[DRU]	3:5	–	U_3O_8	[9]
			Ianthinite	$[U_2^{4+}(UO_2)_4O_6(OH)_4(H_2O)_4](H_2O)_5$	[10]
			Spriggite	$Pb_3[(UO_2)_6O_8(OH)_2](H_2O)_3$	[11]
			Wyartite	$CaU^{5+}(UO_2)_2(CO_3)O_4(OH)(H_2O)_7$	[12]
			Meta-wyartite	$CaU^{5+}(UO_2)_2(CO_3)O_4(OH)(H_2O)_3$	[13]
			Rameauite	$K_2Ca[(UO_2)_6O_6(OH)_4](H_2O)_6$	[14]
Fourmarierite	[DUPUDP]	4:7	Fourmarierite	$Pb[(UO_2)_4O_3(OH)_4](H_2O)_4$	[15]
			Schoepite	$[(UO_2)_8O_2(OH)_{12}](H_2O)_{12}$	[16]
			Metaschoepite	$[(UO_2)_8O_2(OH)_{12}](H_2O)_{10}$	[17]
Vandendriesscheite	[PDUPUPUPUDPDPD]	10:17	Vandendriesscheite	$Pb_{1.5}[(UO_2)_{10}O_6(OH)_{11}](H_2O)_{11}$	[18]
Gauthierite	[UDPDPDUPUP]	7:12	Gauthierite	$KPb[(UO_2)_7O_5(OH)_7](H_2O)_8$	[19]
Sayrite	[RUPURDPD]	5:8	Sayrite	$Pb_2[(UO_2)_5O_6(OH)_2](H_2O)_4$	[20]
Wölsendorfite	[DRUDRUDRUPUPURDUR DURDPDP]	14:23	Wölsendorfite	$Pb_{6.16}Ba_{0.36}[(UO_2)_{14}O_{19}(OH)_4](H_2O)_{12}$	[21]
Curite	$(UD)_6(U^m)_6$	8:14	Curite	$Pb_3(H_2O)_2[(UO_2)_8O_8(OH)_6](H_2O)_1$	[22]
Vandenbrandeite	[URDRRR]	1:4	Vandenbrandeite	$Cu[(UO_2)(OH)_4]$	[23]

[1] Loopstra (1977); [2] Pagoaga *et al.* (1987); [3] Finch *et al.* (2006); [4] Burns & Li (2002); [5] Burns (1999); [6] Cahill & Burns (2000); [7] Burns & Hanchar (1999); [8] Burns (1998b); [9] Loopstra (1970); [10] Burns *et al.* (1997b); [11] Brugger *et al.* (2004); [12] Burns & Finch (1999); [13] Hawthorne *et al.* (2006); [14] Plášil *et al.* (2016); [15] Li & Burns (2000b); [16] Finch *et al.* (1996); [17] Weller *et al.* (1999); [18] Burns (1997); [19] this work; [20] Piret *et al.* (1983); [21] Burns (1999); [22] Li & Burns (2000a); [23] Rosenzweig & Ryan (1977).

Classification of the International Mineralogical Association (IMA2016-004). The description of the new mineral is based on one holotype specimen deposited in the collections of the Natural History Museum of Los Angeles County, 900 Exposition Boulevard, Los Angeles, CA 90007, USA, catalogue number 65644.

Here, we provide a mineral description, including a description of its crystal structure, which presents a topologically new sheet of uranyl polyhedra.

2. Occurrence

Gauthierite was found on a specimen of uraninite–quartz gangue from the Shinkolobwe mine, Shaba province, Democratic Republic of Congo, Africa. The Shinkolobwe mine is best known for the variety of rare secondary uranium minerals found there (*e.g.*, Gauthier *et al.*, 1989), and for its strategic supply of U-ore during the Manhattan Project of WWII. The Shinkolobwe mine is the type locality for more than 25 minerals, several of which have only been found there.

Gauthierite is a rare mineral, having been found only on several specimens. The holotype is a small specimen ($2 \times 1 \times 1$ cm) collected by the late Gilbert Gauthier and provided by him to one of the authors (VB). The mineral assemblage on the sample is soddyite, sklodowskite and an intermediate member of the metazeunerite–metatorbernite series. The matrix is quartz gangue with disseminated altered uraninite, and gauthierite is presumably formed by the combination of radiogenic lead and uranium from altered uraninite, with K leached from other gangue minerals.

3. Physical and optical properties

Gauthierite forms yellowish-orange thick blades, with pronounced lengthwise striations, up to 1 mm in length (Figs. 1 and 2). Crystals are elongated on [0 0 1] and have pyramidal terminations. Crystal forms include {1 0 0}, {1 0 1}, {2 0 −1}, {3 1 0}, {2 1 0}, {1 2 0} and {0 1 0} (Fig. 3). Twinning was not observed by inspection of the morphology or by examination under crossed polars. Crystals are transparent with a strong vitreous lustre. The mineral has a pale orange streak and is non-fluorescent under both long- and short-wavelength UV. The Mohs hardness is about 3–4 (estimated from behaviour when broken). Crystals are brittle with perfect {0 1 0} cleavage and uneven fracture. The density was not measured because of the paucity of pure material for physical measurements (note that it exceeds the density of a Clerici solution). The calculated density is 5.437 g/cm^3 based on the empirical formula and the measured unit-cell dimensions.

Optically, gauthierite is biaxial (−), with $\alpha = 1.780(5)$, $\beta = 1.815(5)$, $\gamma = 1.825(5)$ (measured in white light). The *2V* angle, measured directly on a spindle stage, is 58(1)°; the calculated *2V* is 55.4°. Dispersion is extreme, $r \gg v$.

Fig. 1. Gauthierite crystals with typical terminations on a matrix of uraninite-bearing quartz gangue with tiny yellow soddyite; field of view 1 mm. Photograph by T. Olds. (Online version in colour.)

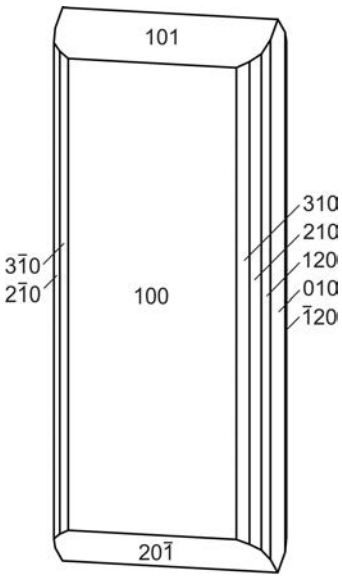

Fig. 2. Crystal drawing of gauthierite, clinographic projection.

The optical orientation is $X = \mathbf{b}$, $Y \approx \mathbf{a}^*$, $Z \approx \mathbf{c}$ (or $X = \mathbf{b}$, $Y \wedge \mathbf{a} = 14°$ in obtuse β). The mineral is pleochroic: X very pale yellow, Y and Z orange-yellow; $X \ll Y \approx Z$.

4. Chemical composition

A crystal aggregate of gauthierite was analyzed using a Cameca SX100 electron microprobe (Masaryk University, Brno), operating in wavelength-dispersive mode with an accelerating voltage of 15 kV, a beam current of 10 nA, and a 10 μm beam diameter. The following X-ray lines and standards were used: $K\alpha$ line for K (sanidine); $M\alpha$ line for Pb (vanadinite), $M\beta$ line for U (uranophane). Other elements, such as Na, Ca, Ba, Cu, Si were also sought, but were below the detection limits (~0.05 to 0.15 wt.% with the analytical conditions used). The counting times were 10–20 s on peak and 50% of this for each background point. Matrix effects were accounted for using the *PAP* correction routine (Pouchou & Pichoir, 1985). Table 2 gives the chemical composition of the gauthierite specimen studied here (9 point analyses). The empirical formula calculated on the basis of 7 U and 34 O atoms *a.p.f.u.* is $K_{0.67}Pb_{0.78}U_7O_{34}H_{23.77}$. The ideal formula is $KPb[(UO_2)_7O_5(OH)_7](H_2O)_8$, which requires K_2O 1.90, PbO 9.00, UO_3 80.74, H_2O 8.35, total 100 wt.%.

Table 2. Results of electron microprobe analyses (in wt.%) of gauthierite.

	Mean ($n = 9$)	Range	S.D.	Standard
K_2O	1.29	1.16–1.38	0.08	Sanidine
PbO	7.17	6.57–7.71	0.33	Vanadinite
UO_3	82.10	81.60–82.44	0.27	Uranophane
H_2O	8.78*			
Total	99.34			
Formula calculated on a basis of 34 O and 7 U atoms				
K	0.67			
Pb	0.78			
U^{6+}	7.00			
H_2O	11.89			

The Gladstone-Dale compatibility index $1 - (K_P/K_C)$ for the empirical formula is −0.062 (fair) and −0.040 (good) for the ideal formula, in both cases using $k(UO_3) = 0.118$, as provided by Mandarino (1976). Note that the $k(UO_3)$ for minerals with uranyl sheet structures is probably in need of revision.

5. Raman and infrared spectroscopy

Data collection of the Raman spectrum of gauthierite was conducted using a Bruker Instruments Sentinel-785 laser head mounted on a Nikon Optiphot-2 microscope. A Peltier-cooled integrated diode laser was calibrated internally with polystyrene and NIST SRM 2065 standards; operated at 400 mW and 785 nm with a 100 μm beam size and 5 cm^{-1} resolution. An attenuated total reflectance (ATR) Fourier transform infrared (FTIR) spectrum was obtained using a liquid N_2-cooled SENSIR Technologies IlluminatIR mounted to an Olympus BX51 microscope. An ATR objective was pressed into crystals of gauthierite and data were collected from 650 to 4000 cm^{-1}. Spectral manipulation was done using Omnic spectral software (Thermo Scientific).

Raman and infrared spectra are given in Figs. 3 and 4, respectively. An infrared band (IR) at 3350 cm^{-1} is assigned to the νO–H of the hydrogen-bonded hydroxyls and that at 3154 cm^{-1} to the νO–H of the hydrogen-bonded water molecules. The IR bands at 2919 and 2852 cm^{-1} are probably related to organic impurities. Approximate O□O distances, corresponding to those in hydrogen-bonded H_2O molecules, were inferred from the energies of the stretching O–H vibrations using the correlation of Libowitzky (1999) and vary around 2.8–2.9 Å. This is in line with the O□O distances obtained from the structure refinement (Table 7). A broad IR band at 1980 cm^{-1} may arise from some overtones or

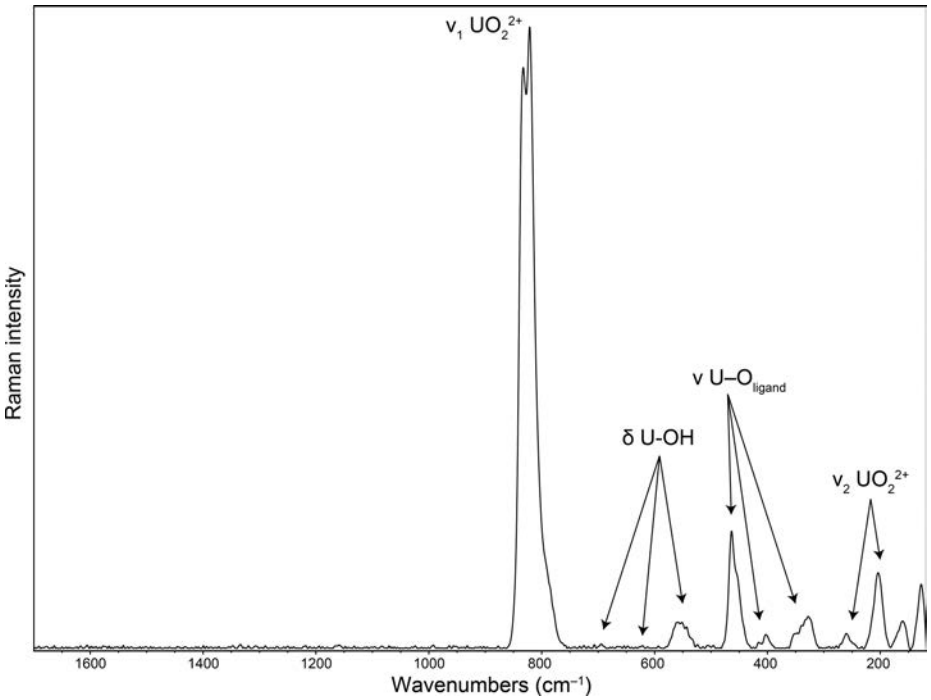

Fig. 3. Raman spectrum of gauthierite collected with 780 nm laser.

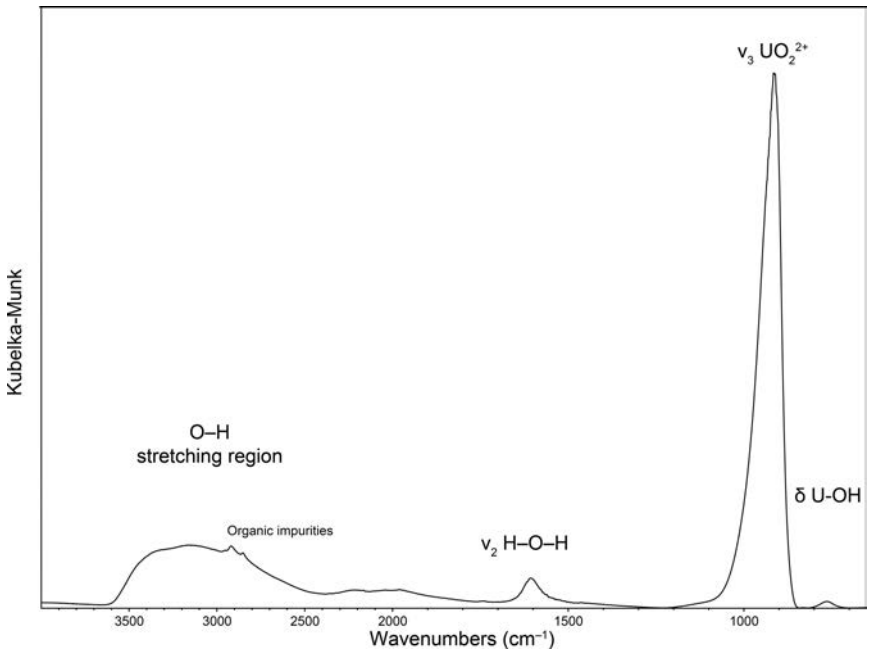

Fig. 4. The infrared (ATR) spectrum of gauthierite.

combination bands. An IR band at 1607 cm^{-1} is assigned to the ν_2 (δ) bending vibrations of water molecules. A very strong IR band at 915 cm^{-1} is attributed to the ν_3 $(UO_2)^{2+}$ antisymmetric stretching vibration and that at 764 cm^{-1} to the libration of water molecules or to δ U–OH bending vibrations. A band arising from the ν_1 $(UO_2)^{2+}$ was not observed in the IR spectrum. The approximate U–O bond length of the uranyl ion inferred from the IR spectrum using an empirical relation (Bartlett & Cooney, 1989) is ~1.77 Å. Raman bands at 833 and 821 cm^{-1} are due to ν_1 $(UO_2)^{2+}$ symmetric stretching vibrations and those at 696, 558 and 539 cm^{-1} are assigned to δ U–OH bending vibrations and/or libration modes of water molecules. The approximate U–O bond lengths of the uranyl ions inferred from the Raman spectrum using an empirical relation (Bartlett & Cooney, 1989) are ~1.78 and ~1.79 Å. Raman bands at 464, 454, 403, 355 and 328 cm^{-1} may be attributed to the ν U–O_{ligand} vibrations, and those at 260 and 204 cm^{-1} to the split doubly degenerate ν_2 (δ) $(UO_2)^{2+}$

Table 3. X-ray powder diffraction data (d in Å) for gauthierite.

I_{obs}	d_{obs}	d_{calc}	I_{calc}	h	k	l	I_{obs}	d_{obs}	d_{calc}	I_{calc}	h	k	l
49	7.28	7.2989	100	0	2	0	23	2.0012	2.0114	14	6	6	2
		7.2568	3	4	0	0			2.0035	6	−2	6	4
									1.9945	5	14	2	0
9	6.32	6.4234	2	−4	1	1	14	1.9624	1.9710	9	4	2	6
		6.3519	4	−3	0	2			1.9602	2	−1	4	6
		5.7038	2	2	0	2							
8	4.52	4.5862	2	0	3	1	6	1.9053	1.9386	2	11	4	2
		4.4952	2	−4	2	2			1.9108	2	−12	4	4
		4.4757	3	1	3	1			1.8938	2	3	6	4
67	3.566	4.2773	2	−3	3	1	5	1.8164	1.8247	4	0	8	0
		3.6494	28	0	4	0			1.8027	5	14	4	0
		3.5766	37	−8	0	2	17	1.7831	1.7877	4	12	0	4
		3.5315	17	−2	0	4			1.7858	8	−10	4	6
100	3.192	3.4738	2	−8	1	2	8	1.7337	1.7369	7	−16	2	4
		3.2109	65	6	2	2			1.7163	2	−4	2	8
		3.1790	28	−2	2	4				2	1	0	8
5	2.775	3.1600	4	−1	2	4	6	1.6799	1.6892	2	9	0	6
		2.7879	6	3	2	4			1.6868	2	16	0	2
		2.6972	2	10	2	0			1.6595	3	−9	2	8
18	2.541	2.5544	15	−8	4	2	8	1.6428	1.6460	3	9	2	6
		2.5378							1.6435				
3	2.436	2.4330	8	−2	4	4	10	1.6130	1.6254	5	−8	8	2
			4	0	6	0			1.6211	3	−2	8	4
			3	−1	0	6			1.6185	3	−18	2	2
4	2.316	2.3238	2	11	0	2			1.6054	4	12	4	4
		2.2882											
3	2.236	2.2429	2	−12	0	4	6	1.5742	1.5781	2	14	6	0
		2.2146	2	−5	2	6			1.5667	3	−10	6	6
7	2.0717	2.1432	2	8	2	4	7	1.5282	1.5329	3	1	4	8
		2.0734	6	14	0	0			1.5312	2	9	4	6
		2.0514	2	1	7	1			1.5107	2	16	4	2
14	2.0426	2.0470	10	4	0	6							

bending vibrations. Raman bands at 160 and 128 cm^{-1} are due to lattice vibrations: $(UO_2)^{2+}$ translations and rotations (Čejka *et al.*, 1998). Note that Raman bands related to the ν_3 $(UO_2)^{2+}$ were not observed in the Raman spectrum.

6. X-ray crystallography

6.1. Powder diffraction

Powder X-ray studies were carried out using a Rigaku R-Axis Rapid II curved imaging plate microdiffractometer with monochromatized Mo$K\alpha$ radiation; a Gandolfi-like motion on the ϕ and ω axes was used to randomize the sample. Observed d spacings and intensities were derived by profile fitting using JADE 2010 software. Data are given in Table 3. Unit-cell parameters refined from the powder data using JADE 2010 with whole-pattern fitting are as follows: (for the monoclinic space group $P2_1/c$) $a = 29.842(5)$ Å, $b = 14.563(5)$ Å, $c = 14.088(5)$ Å, $\beta = 103.906(6)°$ and $V = 5943(3)$ Å^3.

6.2. Single-crystal X-ray diffraction

The single-crystal study was done on an Oxford Gemini diffractometer with an Atlas S2 CCD. A prismatic $0.20 \times 0.11 \times 0.05$ mm crystal was selected for the diffraction experiment and was irradiated using graphite-mono-

Table 4. Summary of data collection conditions and refinement parameters for gauthierite.

Formula	$U_7Pb_{0.94}K_{0.78}O_{32}$
Crystal system	Monoclinic
Space group	$P2_1/c$
Unit-cell parameters: *a*, *b*, *c* [Å]	29.844(2), 14.5368(8), 14.0406(7)
β [°]	103.708(6)
Unit-cell volume [Å^3]	5917.8(6)
Z	8
Calculated density [g/cm^3]	5.394 (for the above mentioned formula)
Crystal size [mm]	0.20 × 0.11 × 0.05
Diffractometer	Oxford Diffraction Gemini with Atlas S2 CCD
Temperature [K]	298
Radiation, wavelength [Å]	Mo*K*α, 0.71073 (50 kV, 30 mA)
θ range for data collection [°]	3.33–29.57
Limiting Miller indices	$h = -26 \rightarrow 37$, $k = -14 \rightarrow 20$, $l = -19 \rightarrow 17$
Axis, frame width (°), time per frame (s)	ω, 1.0, 150
Total reflections collected	34,210
Unique reflections	14,371
Unique observed reflections, criterion	6997, [$I > 3\sigma(I)$]
Absorption coefficient [mm^{-1}], type	43.61; Gaussian integration
T_{min}/T_{max}	0.039/0.385
Data completeness to θ_{max} (%), R_{int}	99.13, 0.070
Structure refinement	Full-matrix least-squares on F^2
No. of param., restraints, constraints	443, 0, 0
R, *wR* (obs)	0.0567, 0.1049
R, *wR* (all)	0.1297, 0.1379
GOF obs/all	1.14, 1.04
Weighting scheme, weights	σ, $w = 1/(\sigma^2(I) + 0.0002119936I^2)$
Largest diffraction peak and hole (e$^-$/Å^3)	8.41 (0.91 Å from U14 atom), −4.88
Twin law; twin fractions	$\begin{pmatrix} 1 & 0 & 1 \\ 0 & 1 & 0 \\ 0 & 0 & -1 \end{pmatrix}$; 0.6004(13), 0.3996(13)

chromatized Mo*Kα* radiation (λ = 0.71073 Å) from a conventional X-ray tube. Gauthierite is monoclinic, with $a = 29.844(2)$ Å, $b = 14.5368(8)$ Å, $c = 14.0406(7)$ Å, $\beta = 103.708(6)°$, $V = 5917.8(6)$ Å^3 and $Z = 8$. A highly redundant dataset was collected, comprising 34,210 reflections. Integration of the data, including corrections for background, polarization and Lorentz effects, was carried out with the CrysAlis *RED* program. The absorption correction, Gaussian integration and an empirical frame-scaling, was done using Jana2006 (Petříček *et al.*, 2014). The details of the crystallography, physical properties, and data-collection details are given in Table 4.

The structure of gauthierite was solved by the charge-flipping algorithm using the Shelxt program (Sheldrick, 2015), giving the most reasonable solution in space-group $P2_1/c$, which was indicated by the systematic absences of reflections. The structure was refined in the Jana2006 program (Petříček *et al.*, 2014) by least-squares on the basis of F^2. However, the diffraction pattern is affected by numerous effects that made the analysis difficult. Amongst other difficulties, the diffraction pattern exhibits rather pseudo-orthorhombic symmetry, and a contribution from several different crystal domains (split crystal). The orthorhombic super-cell, $a = 14.04$, $b = 14.54$, $c = 57.99$, $\alpha = 90°$, $\beta = 90.10°$, $\gamma = 90°$, allows indexing of all observed reflections from both twin domains. Twinning by reticular-merohedry (represented by the 180° rotation around the monoclinic axis), represented by the twin matrix (1 0 1/0 1 0/0 0 −1), was introduced into the refinement, and led to a significant drop in the R_{obs} value of about 10%. The missing O atoms of the structural units and Pb and O atoms located in the interlayer were found in difference Fourier maps; localization of H atoms was not possible. The final cycles of the refinement, including refinement of the site-occupancies of the interstitial cationic sites, converged smoothly to $R = 0.0567$ and $wR = 0.1049$ for 6997 reflections with [$I > 3\sigma(I)$] (GoF = 1.14). Final atom coordinates, displacement parameters and bond valence (BV) sums are given in Table 5, anisotropic displacement parameters are in Table 6, and selected interatomic distances are in Table 7. The crystallographic information file (cif) is provided as Supplementary Material linked to this article and freely available from the the GSW website of the journal: http://eujmin.geoscienceworld.org/.

7. Description of the crystal structure

7.1. Cation coordination

There are fourteen symmetrically non-equivalent U sites in the structure of gauthierite. Each U site is surrounded by seven O ligands forming squat UO_7 pentagonal bipyramids. The two apical O atoms of each bipyramid form short bonds with the U atom, and this unit comprises

Table 5. Atomic positions, displacement parameters (U_{eq}, U_{iso}, in Å^2), occupation factors and bond-valence sums (in valence units, *vu*) for the crystal structure of gauthierite.

Atom	Occ.	*x*	*y*	*z*	U_{eq}/U_{iso}*	∑BV
U1		0.85482(6)	0.24850(10)	0.43940(8)	0.0148(4)	6.02
U2		1.06477(6)	0.24559(8)	0.30101(10)	0.0123(4)	6.17
U3		0.43536(5)	0.75472(8)	0.73056(9)	0.0127(4)	5.99
U4		0.64714(6)	0.73698(7)	1.08167(8)	0.0112(4)	5.85
U5		0.72694(5)	0.72203(6)	0.83577(8)	0.0112(4)	5.98
U6		0.77406(6)	0.24920(9)	0.61214(9)	0.0135(4)	5.88
U7		0.77863(5)	0.74667(8)	1.10956(9)	0.0099(4)	5.93
U8		0.98805(6)	0.27598(7)	0.48153(9)	0.0168(5)	6.10
U9		0.56736(5)	0.74431(8)	0.76117(10)	0.0132(4)	5.95
U10		0.72244(6)	0.26599(7)	0.83780(10)	0.0158(4)	6.23
U11		0.64447(6)	0.26717(7)	1.08089(8)	0.0127(4)	6.01
U12		0.93271(5)	0.24946(8)	0.19835(10)	0.0125(4)	6.16
U13		0.85774(5)	0.75817(9)	0.92996(8)	0.0112(4)	5.96
U14		0.51114(6)	0.76961(8)	0.48810(9)	0.0197(5)	6.09
Pb1	0.976(5)	0.77705(7)	0.49922(8)	0.45695(11)	0.0279(6)	2.06
Pb2	0.386(6)	0.5029(2)	0.5008(3)	0.3656(3)	0.062(2)	1.44
Pb3	0.171(7)	0.6508(9)	1.0060(10)	0.7747(14)	0.122(11)	1.09
Pb4	0.351(6)	0.9362(2)	0.4938(3)	1.0314(4)	0.047(2)	1.56
K1	0.42(3)	0.7074(10)	0.5087(13)	0.9946(14)	0.044(11)	0.89
K2	0.64(5)	0.8077(12)	0.4957(15)	0.794(3)	0.22(3)	0.59
K3	0.50(3)	0.6396(9)	0.5140(13)	0.735(2)	0.082(12)	0.91
O1		1.0199(11)	0.5046(15)	1.1339(18)	0.037(7)*	0.15
O2		0.7190(8)	0.7491(12)	0.6794(13)	0.009(4)*	2.14
O3		0.9940(10)	0.2524(14)	0.3286(15)	0.020(5)*	2.08
O4		1.0055(8)	0.2972(11)	0.6545(13)	0.009(4)*	1.42
O5		0.8506(11)	−0.0241(16)	0.1231(18)	0.042(7)*	0.23
O6		0.8448(17)	0.487(2)	1.090(3)	0.091(13)*	0.04
O7		1.0678(8)	0.3012(12)	0.4729(14)	0.014(4)*	1.38
O8		0.9825(9)	0.3973(13)	0.4632(16)	0.025(5)*	1.67
O9		0.7926(8)	0.7164(11)	0.9590(13)	0.007(4)*	2.06
O10		0.4298(9)	0.8684(13)	0.7725(16)	0.025(5)*	1.81
O11		0.5728(13)	0.5071(18)	0.539(2)	0.056(8)*	0.18
O12		0.9205(9)	0.1316(13)	0.2202(15)	0.022(5)*	1.64
O13		0.6087(11)	0.5054(16)	0.9132(19)	0.044(7)*	0.12
O14		0.5771(12)	0.4878(16)	1.113(2)	0.043(8)*	0.03
O15		0.8356(9)	0.8749(12)	0.9173(14)	0.017(5)*	1.80
O16		0.5963(9)	0.6988(12)	0.9271(13)	0.014(4)*	1.24
O17		0.8800(9)	0.6444(12)	0.9401(14)	0.021(5)*	1.78
O18		0.8548(11)	0.2223(14)	0.6182(18)	0.041(7)*	1.42
O19		0.9844(12)	0.5124(16)	0.312(2)	0.043(7)*	0.00
O20		0.9401(10)	0.3699(13)	0.1764(15)	0.025(5)*	1.70
O21		0.6958(11)	0.4844(15)	0.4792(18)	0.037(7)*	0.33
O22		0.7048(9)	0.6962(13)	0.9867(15)	0.025(5)*	1.40
O23		0.7235(9)	0.8445(11)	0.8568(14)	0.016(5)*	1.73
O24		0.8030(8)	0.7075(11)	0.7796(13)	0.009(4)*	1.36
O25		0.9230(9)	0.2738(13)	0.5357(15)	0.016(5)*	2.12
O26		1.0599(9)	0.3603(13)	0.2560(16)	0.021(5)*	1.70
O27		0.5738(9)	0.7536(14)	0.6004(16)	0.022(5)*	2.08
O28		1.0707(8)	0.1302(11)	0.3445(13)	0.010(4)*	1.77
O29		0.7705(11)	0.1254(15)	0.6354(17)	0.035(6)*	1.55
O30		0.9072(9)	0.2892(13)	0.3374(14)	0.016(5)*	1.32
O31		0.5013(13)	0.6472(16)	0.5017(18)	0.045(7)*	1.68
O32		1.1021(11)	0.1976(14)	0.1892(16)	0.033(6)*	1.24
O33		0.5535(9)	0.6245(12)	0.7388(15)	0.022(5)*	1.76
O34		1.1411(10)	0.2825(12)	0.3881(15)	0.024(5)*	1.37
O35		0.6419(12)	0.2151(14)	0.7583(17)	0.040(6)*	1.33
O36		0.8717(10)	0.1310(14)	0.4300(16)	0.033(6)*	1.77
O37		0.6466(10)	0.8555(12)	1.0450(15)	0.025(5)*	1.65
O38		0.7837(9)	0.2163(11)	0.4583(14)	0.013(4)*	2.07
O39		0.8380(10)	0.3682(14)	0.4377(16)	0.033(6)*	1.81
O40		0.7926(8)	0.6294(12)	1.1458(14)	0.013(5)*	1.64
O41		0.7300(10)	0.1459(13)	0.8396(17)	0.034(6)*	1.93

Table 5. (continued).

Atom	Occ.	x	y	z	U_{eq}/U_{iso}*	∑BV
O42		0.9959(10)	0.1577(13)	0.5058(16)	0.024(6)*	1.84
O43		0.5187(10)	0.8897(13)	0.4804(16)	0.025(5)*	1.73
O44		0.7678(8)	0.8649(12)	1.0743(13)	0.015(5)*	1.88
O45		0.7297(9)	0.5994(12)	0.8203(15)	0.024(5)*	1.80
O46		0.7141(9)	0.2675(13)	0.6781(15)	0.020(5)*	2.15
O47		0.6461(9)	0.7055(10)	0.7561(12)	0.009(4)*	1.40
O48		0.6591(11)	0.3868(14)	1.0949(17)	0.034(6)*	1.72
O49		0.4970(11)	0.5235(15)	0.1739(18)	0.038(6)*	0.09
O50		0.6474(10)	0.6165(11)	1.1130(14)	0.017(4)*	1.66
O51		0.6306(12)	0.1508(16)	1.0644(19)	0.046(8)*	1.83
O52		0.7788(10)	0.3701(13)	0.5888(15)	0.024(5)*	1.90
O53		0.4375(10)	0.6395(14)	0.6884(17)	0.032(6)*	1.74
O54		0.5073(11)	0.7445(14)	0.3317(18)	0.034(6)*	2.09
O55		0.8019(9)	0.2880(12)	0.7826(14)	0.016(5)*	1.33
O56		0.4960(9)	0.7986(12)	0.6446(14)	0.020(5)*	1.39
O57		0.9234(12)	0.5134(16)	0.540(2)	0.049(8)*	0.00
O58		0.8879(15)	0.484(2)	1.295(2)	0.074(10)*	0.00
O59		0.3962(9)	0.8078(13)	0.5746(14)	0.022(5)*	1.16
O60		0.5822(9)	0.8633(12)	0.7888(14)	0.021(5)*	1.65
O61		0.5657(9)	0.2016(12)	0.6057(14)	0.019(5)*	1.42
O62		0.7083(11)	0.3857(15)	0.8384(18)	0.045(7)*	1.79
O63		0.6999(12)	0.2342(17)	0.9810(19)	0.051(8)*	1.46
O64		0.7720(11)	0.5018(13)	1.2713(17)	0.032(6)*	0.28

Table 6. Anisotropic displacement parameters (Å^2) for gauthierite.

Atom	U^{11}	U^{22}	U^{33}	U^{12}	U^{13}	U^{23}
U1	0.0117(8)	0.0240(5)	0.0083(6)	0.0006(5)	0.0013(7)	−0.0016(5)
U2	0.0158(9)	0.0162(5)	0.0052(6)	−0.0021(6)	0.0031(6)	−0.0003(4)
U3	0.0113(9)	0.0223(5)	0.0044(6)	−0.0032(5)	0.0015(6)	0.0008(5)
U4	0.0117(8)	0.0163(5)	0.0059(6)	−0.0011(5)	0.0028(7)	−0.0012(4)
U5	0.0143(8)	0.0123(5)	0.0075(5)	−0.0007(5)	0.0037(6)	0.0001(4)
U6	0.0164(8)	0.0179(5)	0.0076(6)	−0.0005(5)	0.0057(6)	0.0018(5)
U7	0.0093(8)	0.0126(5)	0.0091(6)	0.0005(5)	0.0047(6)	−0.0005(4)
U8	0.0283(11)	0.0133(6)	0.0135(6)	−0.0004(5)	0.0145(7)	−0.0003(4)
U9	0.0123(9)	0.0227(5)	0.0053(6)	−0.0035(5)	0.0032(6)	−0.0028(5)
U10	0.0198(9)	0.0175(5)	0.0099(6)	0.0023(5)	0.0030(6)	0.0008(5)
U11	0.0143(9)	0.0143(5)	0.0093(6)	0.0013(5)	0.0024(7)	−0.0010(4)
U12	0.0159(9)	0.0180(5)	0.0040(6)	−0.0023(6)	0.0029(6)	−0.0004(4)
U13	0.0091(8)	0.0178(5)	0.0075(6)	−0.0001(5)	0.0037(6)	−0.0015(4)
U14	0.0291(12)	0.0198(6)	0.0083(5)	0.0015(6)	0.0007(6)	−0.0017(5)
Pb1	0.0351(12)	0.0248(8)	0.0263(8)	−0.0023(6)	0.0122(8)	−0.0017(5)
Pb2	0.085(6)	0.041(3)	0.039(3)	−0.001(3)	−0.027(3)	−0.0044(17)
Pb3	0.13(2)	0.104(12)	0.133(16)	0.014(12)	0.031(16)	0.036(10)
Pb4	0.059(5)	0.038(3)	0.042(3)	0.009(3)	0.011(3)	−0.0045(19)
K1	0.07(2)	0.045(13)	0.025(11)	0.007(11)	0.035(13)	−0.002(8)
K2	0.10(4)	0.068(17)	0.42(7)	0.005(17)	−0.06(4)	−0.02(2)
K3	0.024(16)	0.051(13)	0.16(3)	0.030(11)	0.009(17)	0.044(14)

the UO_2^{2+} uranyl ion (see Table 6). The five equatorial O ligands, some of which are OH groups (Table 4; Fig. 5a), complete each of the U coordination polyhedra. The U–O bond-lengths (U–O_{Ur} ~1.8 Å; U–O_{eq} ~2.4 Å) in the UO_7 pentagonal bipyramids in gauthierite (Table 6) are in agreement with the most frequently observed bond-lengths in this type of coordination polyhedra in U^{6+} minerals and compounds (Burns *et al.*, 1997a; Burns, 2005).

There are seven independent interstitial metal cation sites, four of which are occupied by Pb^{2+} and three of which contain K^+ cations. On the basis of the site-scattering refinement, all sites have partial occupancies and there is ordering of the Pb and K atoms at their corresponding sites (due to specific and distinct coordination requirements). The K^+ cations occupy trimer clusters between dimers of Pb^{2+} polyhedra (Fig. 6). The coordination of the Pb^{2+} sites is [9]-fold, with distances from ~2.5 to ~3.3 Å,

Table 7. Selected interatomic distances (in Å) for gauthierite.

U1–O36	1.79(2)	U2–O26	1.777(19)	U3–O10	1.78(2)	U4–O37	1.797(18)
U1–O39	1.81(2)	U2–O28	1.779(17)	U3–O53	1.78(2)	U4–O50	1.806(17)
U1–O18	2.54(3)	U2–O3	2.24(3)	U3–O35^{ii}	2.42(4)	U4–O2^{iii}	2.26(2)
U1–O25	2.19(2)	U2–O4^{i}	2.455(18)	U3–O54^{iii}	2.28(3)	U4–O16	2.400(18)
U1–O30	2.43(3)	U2–O7	2.53(2)	U3–O56	2.48(3)	U4–O22	2.49(3)
U1–O38	2.25(3)	U2–O32	2.24(3)	U3–O59	2.354(19)	U4–O27^{iii}	2.27(3)
U1–O55^{i}	2.445(19)	U2–O34	2.38(3)	U3–O61^{ii}	2.43(2)	U4–O47^{iii}	2.595(18)
$\langle U1–O_{Ur}\rangle$	1.80	$\langle U2–O_{Ur}\rangle$	1.78	$\langle U3–O_{Ur}\rangle$	1.78	$\langle U4–O_{Ur}\rangle$	1.80
$\langle U1–O_{eq}\rangle$	2.37	$\langle U2–O_{eq}\rangle$	2.37	$\langle U3–O_{eq}\rangle$	2.39	$\langle U4–O_{eq}\rangle$	2.40
U5–O23	1.811(16)	U6–O29	1.84(2)	U7–O40	1.800(17)	U8–O8	1.784(19)
U5–O45	1.801(18)	U6–O52	1.799(19)	U7–O44	1.796(17)	U8–O42	1.76(2)
U5–O2	2.187(19)	U6–O18	2.42(3)	U7–O2^{iii}	2.23(3)	U8–O3	2.22(2)
U5–O9	2.288(19)	U6–O38	2.30(2)	U7–O9	2.29(2)	U8–O4	2.380(18)
U5–O22	2.39(2)	U6–O46	2.22(3)	U7–O22	2.56(2)	U8–O7	2.44(2)
U5–O24	2.58(2)	U6–O55	2.407(19)	U7–O24^{iii}	2.418(18)	U8–O25	2.25(3)
U5–O47	2.42(2)	U6–O63^{i}	2.53(3)	U7–O34^{iv}	2.44(3)	U8–O30	2.77(2)
$\langle U5–O_{Ur}\rangle$	1.81	$\langle U6–O_{Ur}\rangle$	1.82	$\langle U7–O_{Ur}\rangle$	1.80	$\langle U8–O_{Ur}\rangle$	1.77
$\langle U5–O_{eq}\rangle$	2.37	$\langle U6–O_{eq}\rangle$	2.38	$\langle U7–O_{eq}\rangle$	2.39	$\langle U8–O_{eq}\rangle$	2.41
U9–O33	1.800(18)	U10–O41	1.759(19)	U11–O48	1.79(2)	U12–O12	1.79(2)
U9–O60	1.805(18)	U10–O62	1.79(2)	U11–O51	1.74(2)	U12–O20	1.80(2)
U9–O16	2.378(18)	U10–O35	2.51(3)	U11–O35^{v}	2.52(3)	U12–O3	2.26(2)
U9–O27	2.31(2)	U10–O38^{v}	2.19(2)	U11–O46^{v}	2.26(2)	U12–O4^{i}	2.49(2)
U9–O47	2.43(3)	U10–O46	2.20(2)	U11–O59^{vi}	2.31(19)	U12–O18^{i}	2.37(3)
U9–O54^{iii}	2.25(3)	U10–O55	2.68(3)	U11–O61^{v}	2.50(3)	U12–O25^{i}	2.26(2)
U9–O56	2.49(2)	U10–O63	2.31(3)	U11–O63	2.46(4)	U12–O30	2.33(2)
$\langle U9–O_{Ur}\rangle$	1.80	$\langle U10–O_{Ur}\rangle$	1.78	$\langle U11–O_{Ur}\rangle$	1.77	$\langle U12–O_{Ur}\rangle$	1.80
$\langle U9–O_{eq}\rangle$	2.37	$\langle U10–O_{eq}\rangle$	2.38	$\langle U11–O_{eq}\rangle$	2.41	$\langle U12–O_{eq}\rangle$	2.34
U13–O15	1.815(18)	U14–O31	1.82(2)				
U13–O17	1.776(19)	U14–O43	1.77(2)				
U13–O7^{iv}	2.40(2)	U14–O16^{viii}	2.90(3)				
U13–O9	2.16(2)	U14–O27	2.15(2)				
U13–O24	2.457(18)	U14–O54	2.20(3)				
U13–O32^{vii}	2.37(3)	U14–O56	2.38(2)				
U13–O34^{iv}	2.57(2)	U14–O61^{ix}	2.40(2)				
$\langle U13–O_{Ur}\rangle$	1.80	$\langle U14–O_{Ur}\rangle$	1.80				
$\langle U13–O_{eq}\rangle$	2.39	$\langle U14–O_{eq}\rangle$	2.41				
Pb1–O5^{v}	2.82(3)	Pb2–O10^{viii}	2.96(2)	Pb3–O14^{viii}	2.76(3)	Pb4–O1	2.57(3)
Pb1–O15^{viii}	2.68(2)	Pb2–O11	2.80(3)	Pb3–O21^{iii}	2.87(3)	Pb4–O1^{xii}	2.92(3)
Pb1–O21	2.53(3)	Pb2–O11^{ix}	2.89(4)	Pb3–O23	3.22(3)	Pb4–O6	3.03(5)
Pb1–O23^{viii}	2.937(18)	Pb2–O31	2.87(3)	Pb3–O35^{xvii}	3.06(3)	Pb4–O17	2.87(2)
Pb1–O39	2.69(3)	Pb2–O31^{ix}	2.87(3)	Pb3–O41^{xvii}	3.09(3)	Pb4–O20^{x}	2.70(2)
Pb1–O41^{i}	2.84(2)	Pb2–O33^{ix}	2.67(2)	Pb3–O48^{viii}	3.03(3)	Pb4–O28^{iv}	2.679(19)
Pb1–O44^{viii}	2.629(19)	Pb2–O49	2.67(3)	Pb3–O50^{viii}	2.87(3)	Pb4–O36^{v}	2.78(2)
Pb1–O52	2.63(2)	Pb2–O53^{ix}	2.92(3)	Pb3–O53^{ii}	3.41(4)	Pb4–O42^{iv}	3.25(3)
Pb1–O64^{x}	2.58(2)	Pb2–O60^{viii}	3.45(2)	Pb3–O60	2.95(3)	Pb4–O42^{v}	2.91(3)
$\langle Pb1–O\rangle$	2.70	$\langle Pb2–O\rangle$	2.90	$\langle Pb3–O\rangle$	3.03	$\langle Pb4–O\rangle$	2.86
K1–O13	2.90(4)	K2–O5^{v}	3.00(6)	K3–O10^{vi}	2.94(3)		
K1–O22	2.73(3)	K2–O17	3.39(4)	K3–O11	3.00(4)		
K1–O29^{i}	3.08(3)	K2–O24	3.09(3)	K3–O13	2.87(4)		
K1–O40	3.39(3)	K2–O36^{v}	3.00(4)	K3–O33	3.04(4)		
K1–O45	2.99(3)	K2–O45	2.87(5)	K3–O37^{viii}	3.32(4)		
K1–O48	2.86(4)	K2–O52	3.34(4)	K3–O45	2.95(3)		
K1–O50	3.14(4)	K2–O55	3.03(3)	K3–O47	2.80(2)		
K1–O62	2.83(3)	$\langle K2–O\rangle$	3.10	K3–O51^{i}	3.35(4)		
$\langle K1–O\rangle$	2.99			K3–O62	2.89(3)		
				$\langle K3–O\rangle$	3.02		
O1–O12^{iv}	3.01(3)	O6–O17	3.43(5)	O13–O14	3.18(4)	O19–O20	2.91(3)
O1–O19^{xi}	2.94(4)	O6–O18^{v}	3.08(4)	O13–O16	2.85(3)	O19–O26	3.38(4)
O1–O20^{xi}	3.25(4)	O6–O20^{xi}	3.29(5)	O13–O33	3.13(3)	O19–O28^{xviii}	2.96(3)

Table 7. (continued).

O1–O26^{xi}	2.79(3)	O6–O28^{iv}	3.23(5)	O13–O43^{iii}	3.41(4)	O19–O57^{vii}	3.05(4)
O1–O28^{iv}	3.33(4)	O6–O29^{v}	2.95(6)	O13–O48	3.15(3)	O19–O58^{x}	2.86(6)
O1–O42^{iv}	2.93(3)	O6–O36^{v}	3.08(5)	O13–O49^{ix}	3.13(4)	O21–O23^{viii}	3.24(3)
O1–O42^{v}	2.95(3)	O6–O40	2.81(5)	O13–O50	3.20(3)	O21–O37^{viii}	3.01(4)
O5–O12	3.16(3)	O6–O58	2.87(5)	O13–O59^{vi}	2.88(3)	O21–O41^{i}	3.07(4)
O5–O15^{xiii}	3.18(3)	O11–O31	2.91(4)	O14–O43^{vi}	3.19(4)	O21–O44^{viii}	3.14(3)
O5–O26^{xiv}	3.27(4)	O11–O31^{ix}	3.11(4)	O14–O43^{iii}	2.85(3)	O21–O51^{i}	3.19(4)
O5–O34^{xiv}	2.83(3)	O11–O33	3.45(4)	O14–O48	2.92(4)	O21–O52	3.07(4)
O5–O39^{i}	3.40(3)	O11–O37^{viii}	2.96(4)	O14–O49^{xi}	2.77(5)	O21–O63^{i}	3.18(3)
O5–O44^{xiii}	2.89(4)	O11–O51^{i}	2.84(4)	O14–O50	2.81(4)	O49–O53^{ix}	3.37(3)
O5–O52^{i}	3.06(4)			O14–O53^{xvi}	3.45(4)	O49–O56^{viii}	2.62(3)
O5–O57^{i}	2.70(5)			O14–O60^{iii}	3.26(3)	O49–O60^{viii}	3.14(3)
				O14–O61^{v}	2.77(3)	O57–O58^{x}	3.37(4)
						O58–O64	3.41(5)

Symmetry codes: (i) $x, -y+1/2, z-1/2$; (ii) $-x+1, y+1/2, -z+3/2$; (iii) $x, -y+3/2, z+1/2$; (iv) $-x+2, y+1/2, -z+3/2$; (v) $x, -y+1/2, z+1/2$; (vi) $-x+1, y-1/2, -z+3/2$; (vii) $-x+2, -y+1, -z-1$;(viii) $x, -y+3/2, z-1/2$; (ix) $-x+1, -y+1, -z+1$; (x) $x, y, z-1$;(xi) $x, y, z+1$; (xii) $-x+2, -y+1, -z+2$; (xiii) $x, y-1, z-1$; (xiv) $-x+2, y-1/2, -z+1/2$; (xv) $-x+2, y-1/2, -z+3/2$; (xvi) $-x+1, -y+1, -z+2$; (xvii) $x, y+1, z$; (xviii) $-x+2, y+1/2, -z+1/2$; (xix) $-x+1, -y+2, -z+1$; (xx) $-x+1, y+1/2, -z+1/2$.

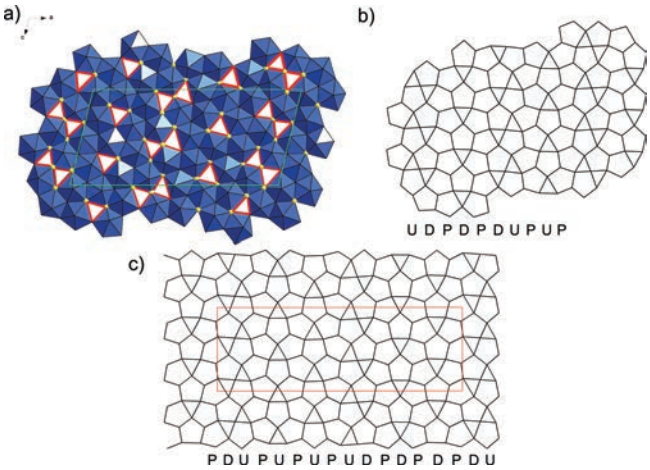

Fig. 5. The structural sheet of $[(UO_2)_7O_5(OH)_7]^{3-}$ composition in the structure of gauthierite. (a) With the (OH) sites displayed (yellow); unit-cell edges are in green. (b) Graphical representation of the gauthierite anion-topology with the chain sequence. (c) Graphical representation of the vandendriesscheite anion-topology with the chain sequence. (Online version in colour.)

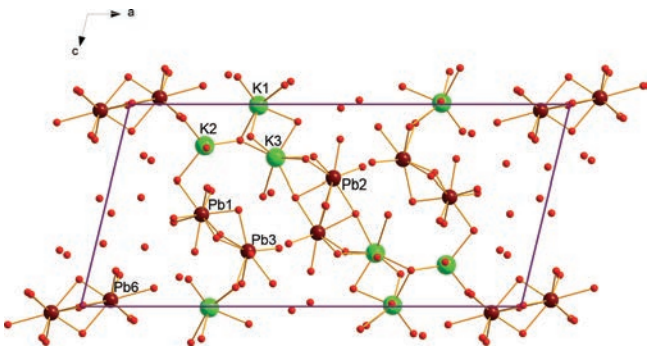

Fig. 6. Interstitial complex in the structure of gauthierite viewed along [0 1 0]. Unit-cell edges outlined in solid purple lines. (Online version in colour.)

consistent with activity of the $6s^2$ lone-electron pairs on Pb^{2+}. The coordination of the K^+ sites ranges from [7]- to

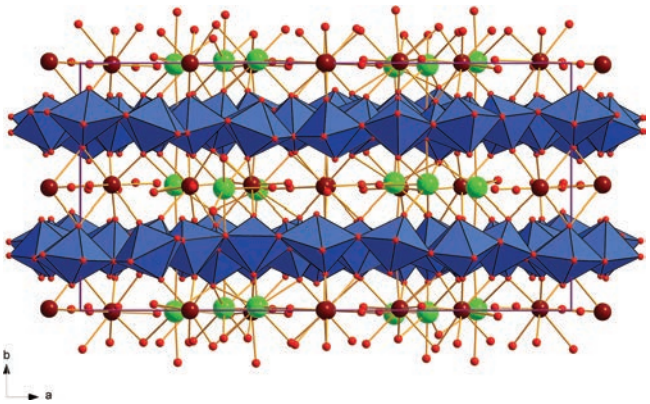

Fig. 7. The structure of gauthierite viewed along [0 0 1], perpendicular to the stacking. The sheets of uranyl pentagonal bipyramids (blue) alternate with interlayer K (green) and Pb (violet) atoms and molecular H_2O. Unit-cell edges outlined in solid purple lines. (Online version in colour.)

[9]-fold with bond-distances from ~2.7 to ~3.4 Å. The interstitial cations are linked to interlayer H_2O molecules and O atoms within the sheets of uranyl pentagonal bipyramids. The interstitial complex contains eight H_2O molecules. Only six H_2O sites were located, but two additional H_2O *pfu* are inferred based upon the residual electron density.

7.2. Structure connectivity

The uranyl pentagonal bipyramids share edges and vertices to form a sheet of polyhedra that is parallel to (0 1 0) (Fig. 5a). Adjacent structure sheets (Fig. 7) are linked through apical O_{Ur} atoms by the Pb- and K-polyhedra and a H-bond network that involves interstitial H_2O groups and O sites and OH groups within the sheets. The stacking distance is represented by the **b** periodicity of the lattice and corresponds to ~14.5 Å.

7.3. Bond-valence analysis and structure formula

The calculated bond-valence sums for the gauthierite structure based on the refined interatomic distances and bond-valence parameters given by Burns *et al.* (1997a) and by Krivovichev & Brown (2001) for U^{6+}–O and Pb^{2+}–O pairs, respectively, are given in Table 5. There are numerous O sites within the sheet that correspond to OH. The number of O sites that are protonated is consistent with charge-balance requirements arising from the charge of the interstitial complex. The ideal formula of gauthierite, considering the bond-valence analysis, is KPb $[(UO_2)_7O_5(OH)_7](H_2O)_8$.

7.4. Topology of the structure sheets

The sheets of uranyl pentagonal bipyramids in gauthierite are topologically unique (Fig. 5b), although they to some extent resemble those of vandendriesscheite (Burns, 1997) (Fig. 5c). Using the formalism of chain stacking sequences proposed by Miller *et al.* (1996), it is apparent that, although the gauthierite and vandendriesscheite sheets are both based upon stacking of the **U**, **D** and **P** chains, the sequence is shorter in the case of gauthierite. For gauthierite the sequence is **UDPDPDUPUP**, whereas for vandendriesscheite the sequence is **PDUPUPUPUDPDPDPDUPUP** (Fig. 5b, c). The longer chain stacking sequence in vandendriesscheite is reflected in the larger cell dimensions, having $b \sim 41$ Å, which corresponds to the stacking length of the sheet (Burns, 1997). The sheet in gauthierite is a novel uranyl sheet topology, which is designated as the *gauthierite topology*; the chain stacking sequence is $P_4(UD)_6$.

7.5. The role and the typology of H_2O in the gauthierite structure

We were able to identify seven OH groups within the sheets of uranyl pentagonal bipyramids and six H_2O groups in the interlayer space (and we assume two additional molecules) where suggested by local bond-valence requirements. The types and particular roles of H_2O in the structures of hydrated oxysalts have been described and reviewed in detail elsewhere (Hawthorne, 1992, 2012; Hawthorne & Schindler, 2008; Hawthorne & Sokolova, 2012; Schindler & Hawthorne, 2008). Several details of the types and roles of the H_2O groups can be identified on the basis of the bond-valence approach (Schindler & Hawthorne, 2008). Among the (H_2O) groups in the structure of gauthierite, the majority is ascribed to non-transformer or inverse-transformer (H_2O). According to Schindler & Hawthorne (2008), the O atom in the non-transformer (H_2O) group has coordination number [4], and thus serves as a propagator of the bond-valence from interstitial cations to the anions within the structural units. Such O atoms would have BV sums (without contributions of the H-bonds) close to 0-0.1 *vu*. Such O atoms in gauthierite are linked to two H atoms (2×0.8 *vu*) and two interstitial cations, or one cation and receive one H-bond (~0.2 *vu*) from an (OH) group localized on the structure sheet. Some of the (H_2O) in the structure are inverse-transformer (H_2O) groups, and are [5]-coordinate. This type of (H_2O) has a similar role as transformer (H_2O): to transform (weak) bond-valence from cations and transfer it to anions. The expected bond-valence sums of the O atom within such a group should be ~0.15–0.40 *vu*.

8. Discussion – Comparison to other uranyl-oxide hydroxy-hydrate minerals

The crystal chemistry of uranyl-oxide hydroxy-hydrate minerals was discussed in detail from the point of view of the bond-valence approach by Schindler & Hawthorne (2004). We refer to that paper and Schindler & Hawthorne (2008) for details. As mentioned above, the gauthierite sheet is topologically related to vandendriesscheite (Burns, 1997). We will document that this implies some important characteristics of gauthierite. The structural unit of gauthierite, $[(UO_2)_7O_5(OH)_7]^{3-}$, is characterized by a charge-deficiency per anion (*CDA*) of 0.17 *vu*. This is a slightly larger value than calculated for vandendriesscheite (0.14 *vu*), and lower than for four-marierite (0.19 *vu*) (values from Schindler & Hawthorne, 2004). The range of Lewis basicity of the structural unit of gauthierite is 0.14–0.24 *vu*, similar to the above-mentioned minerals. Both vandendriesscheite and four-marierite belong to the early alteration products that form from the oxidation–hydration weathering of uraninite (Finch & Ewing, 1992; Finch & Murakami, 1999; Plášil, 2014). Among the uranyl-oxides they are the first to form, and are characterized by a high molar proportion of H_2O within the structure sheets compared to the molar content of those containing mono-, di- or trivalent cations (Finch & Ewing 1992; Schindler & Hawthorne, 2004; Plášil, 2014). Gauthierite is one of these early-formed alteration phases, and represents an interesting transition between Pb^{2+}- and alkali metals and alkaline earths-containing minerals (*e.g.*, compreignacite or becquerelite).

Acknowledgements: This paper benefited from the constructive reviews of two anonymous referees and editorial work of Sergey Krivovichev. Single-crystal X-ray diffraction experiments were done using instruments of the ASTRA lab established within the Operation program Prague Competitiveness – project CZ.2.16/3.1.00/24510. Involvement of T.A.O. and P.C.B. in this work was funded by the Chemical Sciences, Geosciences and Biosciences Division, Office of Basic Energy Sciences, Office of Science, U.S. Department of Energy, Grant No. DE-FG02-07ER15880. A portion of this study was funded by the John Jago Trelawney Endowment to the Mineral Sciences Department of the Natural History Museum of Los Angeles County. Participation of J.Č. in this study was supported by the Ministry of Culture of the Czech Republic (DKRVO 2016/02; National Museum 00023272).

References

Bartlett, J.R. & Cooney, R.P. (1989): On the determination of uranium-oxygen bond lengths in dioxouranium(VI) compounds by Raman spectroscopy. *J. Mol. Struct.*, **193**, 295–300.

Brugger, J., Krivovichev, S.V., Berlepsh, P., Meisser, N., Ansermet, S., Armbruster, T. (2004): Spriggite, $Pb_3[(UO_2)_6O_8(OH)_2](H_2O)_3$, a new mineral with β-$U_3O_8$-type sheets: description and crystal structure. *Am. Mineral.*, **89**, 339–347.

Brugger, J., Meisser, N., Etschmann, B., Ansermet, S., Pring, A. (2011): Paulscherrerite from the Number 2 Workings, Mount Painter Inlier, Northern Flinders Ranges, South Australia: "dehydrated schoepite" is a mineral after all. *Am. Mineral.*, **296**, 229–240.

Burns, P.C. (1997): A new uranyl oxide hydrate sheet in vandendriesscheite: implications for mineral paragenesis and the corrosion of spent nuclear fuel. *Am. Mineral.*, **82**, 1176–1186.

— (1998a): The structure of richetite, a rare lead uranyl oxide hydrate. *Can. Mineral.*, **36**, 187–199.

— (1998b): The structure of compreignacite, $K_2(UO_2)_3O_2(OH)_3]_2(H_2O)_7$. *Can. Mineral.*, **36**, 1061–1067.

— (1999): A new complex sheet of uranyl polyhedra in the structure of wölsendorfite. *Am. Mineral.*, **84**, 1661–1673.

— (2005): U^{6+} minerals and inorganic compounds: insights into an expanded structural hierarchy of crystal structures. *Can. Mineral.*, **43**, 1839–1894.

Burns, P.C. & Finch, R.J. (1999): Wyartite: crystallographic evidence for the first pentavalent-uranium mineral. *Am. Mineral.*, **84**, 1456–1460.

Burns, P.C. & Hanchar, J. (1999): The structure of masuyite, Pb $[(UO_2)_3O_8(OH)_2](H_2O)_3$, and its relationship to protasite. *Can. Mineral.*, **37**, 1483–1491.

Burns, P.C. & Li, Y. (2002): The structures of becquerelite and Sr-exchanged becquerelite. *Am. Mineral.*, **87**, 550–557.

Burns, P.C., Ewing, R.C., Hawthorne, F.C. (1997a): The crystal chemistry of hexavalent uranium: polyhedron geometries, bond-valence parameters, and polymerization of polyhedra. *Can. Mineral.*, **35**, 1551–1570.

Burns, P.C., Finch, R.J., Hawthorne, F.C., Miller, M.L., Ewing, R.C. (1997b): The crystal structure of ianthinite, $[U^{4+}{}_2(UO_2)_4O_6(OH)_4(H_2O)_4](H_2O)_5$: a possible phase for Pu^{4+} incorporation during the oxidation of spent nuclear fuel. *J. Nucl. Mater.*, **249**, 199–206.

Cahill, C.L. & Burns, P.C. (2000): The structure of agrinierite: a Sr-containing uranyl oxide hydrate mineral. *Am. Mineral.*, **85**, 1294–1297.

Čejka, J., Sejkora, J., Skála, R., Čejka Jr. J., Novotná, M., Ederová, J. (1998): Contribution to the crystal chemistry of synthetic becquerelite, billietite and protasite. *N. Jahrb. Mineral., Abh.,* **174**, 159–180.

Finch, R.J. & Ewing, R.C. (1992): The corrosion of uraninite under oxidizing conditions. *J. Nucl. Mater.*, **190**, 133–156.

Finch, R.J. & Murakami, T. (1999): Systematics and paragenesis of uranium minerals. *in* "Uranium: Mineralogy, Geochemistry and the Environment. Mineralogical Society of America and Geochemical Society", P.C. Burns and R.C. Ewing, eds., *Rev. Mineral. Geochem.*, **38**, 91–179.

Finch, R.J., Cooper, M.A., Hawthorne, F.C., Ewing, R.C. (1996): The crystal structure of schoepite, $[(UO_2)_8O_2(OH)_{12}](H_2O)_{12}$. *Can. Mineral.*, **34**, 1071–1088.

Finch, R.J., Burns, P.C., Hawthorne, F.C., Ewing, R.C. (2006): Refinement of the crystal structure of billietite Ba $[(UO_2)_6O_4(OH)_6](H_2O)_8$. *Can. Mineral.*, **44**, 1197–1205.

Gauthier, G., Armand, F., Deliens, M., Piret, P. (1989): The uranium deposits of the Shaba region, Zaire. *Mineral. Rec.*, **20**, 265–288.

Hawthorne, F.C. (1992): The role of OH and H_2O in oxide and oxysalt minerals. *Z. Kristallogr.*, **201**, 183–206.

— (2012): A bond-topological approach to theoretical mineralogy: crystal structure, chemical composition and chemical reactions. *Phys. Chem. Minerals*, **39**, 841–874.

Hawthorne, F.C. & Sokolova, E. (2012): The role of H_2O in controlling bond topology: I. The $^{[6]}Mg(SO_4)(H_2O)_n$ (n = 0–11) structures. *Z. Kristallogr.*, **227**, 594–603.

Hawthorne, F.C. &Schindler, M. (2008): Understanding the weakly bonded constituents in oxysalt minerals. *Z. Kristallogr.*, **223**, 41–68.

Hawthorne, F.C., Finch, R.J., Ewing, R.C. (2006): The crystal structure of dehydrated wyartite, $Ca(CO_3)(U^{5+}(U^{6+}O_2)_2O_4(OH))(H_2O)_3$. *Can. Mineral.*, **44**, 1379–1385.

Janeczek, J., Ewing, R.C., Oversby, V.M., Werme, L.O. (1996): Uraninite and UO_2 in spent nuclear fuel: a comparison. *J. Nucl. Mater.*, **238**, 121–130.

King, V.T. (2006): Died, Gilbert Gauthier, 81. *Mineral. Rec.*, **37**, 354–355.

Krivovichev, S.V. & Brown, I.D. (2001): Are the compressive effects of encapsulation an artifact of the bond valence parameters? *Z. Kristallogr.*, **216**, 245–247.

Krivovichev, S.V. & Plášil, J. (2013): Mineralogy and crystallography of uranium. *in* "Uranium: From Cradle to Grave", P.C. Burns and G.E. Sigmon, eds., *MAC Short Courses*, **43**, 15–119.

Li, Y. & Burns, P.C. (2000a): Investigations of crystal-chemical variability in lead uranyl oxide hydrates. I. Curite. *Can. Mineral.*, **38**, 727–735.

—, — (2000b): Investigations of crystal-chemical variability in lead uranyl oxide hydrates. II. Fourmarierite. *Can. Mineral.*, **38**, 737–749.

Libowitzky, E. (1999): Correlation of O–H stretching frequencies and O–HLO hydrogen bond lengths in minerals. *Monatsh. Chem.*, **130**, 1047–1059.

Loopstra, B.O. (1970): The structure of β-U_3O_8. *Acta Crystallogr.*, **B26**, 656–657.

— (1977): On the crystal structure of α-U_3O_8. *J. Inorg. Nucl. Chem.*, **39**, 1713–1714.

Mandarino, J.A. (1976): The Gladstone-Dale relationship – Part 1: derivation of new constants. *Can. Mineral.*, **14**, 498–502.

Miller, M.L., Finch, R.J., Burns, P.C., Ewing, R.C. (1996): Description and classification of uranium oxide hydrate sheet anion topologies. *J. Mater. Res.*, **11**, 3048–3056.

Pagoaga, M.K., Appleman, D.E., Stewart, J.M. (1987): Crystal structures and crystal chemistry of the uranyl oxide hydrates becquerelite, billietite, and protasite. *Am. Mineral.*, **72**, 1230–1238.

Petříček, V., Dušek, M., Palatinus, L. (2014): Crystallographic Computing System Jana 2006: general features. *Z. Kristallogr.*, **229**, 345–352.

Piret, P., Deliens, M., Piret-Meunier, J., Germain, G. (1983): La sayrite, $Pb_2[(UO_2)_5O_6(OH)_2]\cdot 4H_2O$, nouveau minéral; propriétés et structure cristalline. *Bull. Minéral.*, **106**, 299–304.

Plášil, J. (2014): Oxidation-hydration weathering of uraninite: the current state-of-knowledge. *J. Geosci.*, **59**, 99–114.

Plášil, J., Škoda, R., Čejka, J., Bourgoin, V., Boulliard, J.-C. (2016): Crystal structure of the uranyl-oxide mineral rameauite. *Eur. J. Mineral.*, doi:10.1127/ejm/2016/0028-2568.

Pouchou, J.L. & Pichoir, F. (1985): "PAP" (ϕρZ) procedure for improved quantitative microanalysis. *in* "Microbeam analysis", J. T. Armstrong, ed. San Francisco Press, San Francisco, 104–106.

Rosenzweig, A. & Ryan, R.R. (1977): Vandenbrandeite $CuUO_2(OH)_4$. *Cryst. Struct. Commun.*, **6**, 53–56.

Schindler, M. & Hawthorne, F.C. (2004): A bond-valence approach to the uranyl-oxide hydroxy-hydrate minerals: chemical composition and occurrence. *Can. Mineral.*, **42**, 1601–1627.

—, — (2008): The stereochemistry and chemical composition of interstitial complexes in uranyl-oxysalt minerals. *Can. Mineral.*, **46**, 467–501.

Sheldrick, G.M. (2015): SHELXT – integrated space-group and crystal-structure determination. *Acta Crystallogr.*, **A71**, 3–8.

Walenta, K. & Theye, T. (2012): Heisenbergite, a new uranium mineral from the uranium deposit of Menzenschwand in the Southern Black Forest, Germany. *N. Jahrb. Mineral., Abh.*, **189**, 117–123.

Weller, M.T., Light, M.E., Gelbrich, T. (1999): Structure of uranium (VI) oxide dihydrate, $UO_3{\cdot}2H_2O$; synthetic meta-schoepite $(UO_2)_4O(OH)_6{\cdot}5H_2O$. *Acta Crystallogr.*, **B56**, 577–583.

Received 25 April 2016
Modified version received 29 May 2016
Accepted 1 September 2016